

Natural quark mass patterns

K. Wang

Department of Physics, University of California, Los Angeles, California 90024

(Received 8 May 1996)

We incorporate the idea of natural mass matrices into the construction of phenomenologically viable quark mass matrix patterns. The general texture pattern for natural Hermitian mass matrices is obtained and several applications of this result are made. [S0556-2821(96)00121-X]

PACS number(s): 12.15.Ff, 12.10.Kt

I. INTRODUCTION

Recently, we proposed the idea of natural mass matrices [1], an organizing principle useful in the construction of phenomenologically viable grand unification theory (GUT) scale quark mass matrix patterns. In this note, we present a detailed implementation and discuss certain applications of this result, among which is the construction of some supersymmetric (SUSY) GUT mass matrix patterns. We begin with a brief summary of the low energy data (LED) which we use as inputs and a discussion of the evolution of these parameters in the minimal supersymmetric standard model (MSSM). This is followed by the introduction of a convenient parametrization of Hermitian mass matrices which, along with the ‘‘naturalness’’ requirement [1], allows us to derive the general texture pattern for natural Hermitian quark mass matrices. The usefulness of this result is then demonstrated through several examples. Specifically, using the expression for this general pattern, we conduct an efficient viability check on a known quark mass pattern, perform an exercise of finding mass patterns with most texture zeros, and finally, we construct some simple, generic mass patterns which may be useful as templates for contemplating ‘‘predictive’’ quark mass *Ansätze*.

II. LED INPUTS AND THEIR EVOLUTION IN MSSM

In our bottom-up approach of constructing quark mass matrices, we use as inputs the quark mass ratios evaluated at $m_t \approx 175$ (GeV) and values of Cabibbo-Kobayashi-Maskawa (CKM) matrix elements in the standard Wolfenstein parametrization.¹

Notice, in particular, the different degrees of experimental uncertainties associated with the LED. Roughly speaking, $\Delta\lambda$ is about 1%, $\Delta A, \Delta\xi_{ct}$ are slightly below $\sim 10\%$ while $\Delta\sigma, \Delta\xi_{ut}, \Delta\xi_{db}, \Delta\xi_{sb}$ are of $\sim 30\%$ and δ is only loosely bounded.

Additionally, one can impose the existing constraints on the relative sizes of the light quark masses from current algebra analyses [2]:

$$\left(\frac{m_u}{m_d}\right)^2 + \frac{1}{Q^2} \left(\frac{m_s}{m_d}\right)^2 = 1, \quad \text{with } Q = 24 \pm 1.6. \quad (1)$$

¹See Ref. [1] for the sources of the numbers summarized in Table I.

According to a recent study [3], the value of Q in the above equation is likely to be somewhat smaller ($Q = 22.7 \pm 0.8$); and the range of values for the quark mass ratios may be even further narrowed down to: $m_u/m_d = 0.553 \pm 0.043$ and $m_s/m_d = 18.9 \pm 0.8$. In terms of the mass ratio parameter ξ 's of Table I, the latter translates to

$$\xi_{db}/\xi_{sb} = 1.09 \pm 0.04. \quad (2)$$

Typically, one wishes to construct mass patterns at some high energy scales as, for instance, one does when building certain GUT models. To do so, using the LED inputs of Table I, one must also take into account the evolution of these parameters. Here, as an example, we consider the scaling behavior of the LED parameters in the MSSM which actually has a rather simple description, provided that the underlying mass matrices are ‘‘natural’’² [1]. Denoting the [3,3] matrix elements of the u -type and d -type Yukawa matrices as λ_u and λ_d , respectively, one has³

$$\xi_{ct}(m_G)/\xi_{ct} \approx \xi_{ut}(m_G)/\xi_{ut} \approx r_u, \quad (3)$$

$$\xi_{sb}(m_G)/\xi_{sb} \approx \xi_{db}(m_G)/\xi_{db} \approx r_d, \quad (4)$$

$$\lambda(m_G)/\lambda \approx \sigma(m_G)/\sigma \approx 1, \quad (5)$$

$$A(m_G)/A \approx r, \quad (6)$$

where the scaling parameters are defined by

$$r_u = \exp\left(-\frac{1}{16\pi^2} \int_{\ln m_t}^{\ln m_G} \{3\lambda_u^2(\mu) + \lambda_d^2(\mu)\} d \ln \mu\right),$$

$$r_d = \exp\left(-\frac{1}{16\pi^2} \int_{\ln m_t}^{\ln m_G} \{\lambda_u^2(\mu) + 3\lambda_d^2(\mu)\} d \ln \mu\right),$$

²Assuming quark and lepton mass matrices are ‘‘natural,’’ the corresponding Yukawa matrices then exhibit a certain definite hierarchy. In particular, the [3,3] matrix elements are much greater than the rest, a fact gainfully exploited in the simplification of solutions to the one-loop renormalization group equations (RGE's) for the Yukawa matrices [4].

³For conciseness, unless otherwise specified, values of the parameters in the expressions below are taken to be those evaluated at m_t .

TABLE I. LED inputs used in quark mass pattern construction.

Quark mass ratios	$m_u/m_t = \xi_{ut}\lambda^7$	$\xi_{ut} = 0.49 \pm 0.15$
	$m_c/m_t = \xi_{ct}\lambda^4$	$\xi_{ct} = 1.46 \pm 0.13$
	$m_d/m_b = \xi_{db}\lambda^4$	$\xi_{db} = 0.58 \pm 0.18$
	$m_s/m_b = \xi_{sb}\lambda^2$	$\xi_{sb} = 0.55 \pm 0.18$
CKM parameters	$V_{us} = \lambda + O(\lambda^7)$	$\lambda = 0.221 \pm 0.002$
	$V_{cb} = A\lambda^2 + O(\lambda^4)$	$A = 0.78 \pm 0.05$
	$V_{ub} = A\sigma\lambda^3 e^{-i\delta}$	$\sigma = 0.36 \pm 0.09, \delta = [45^0, 158^0]$

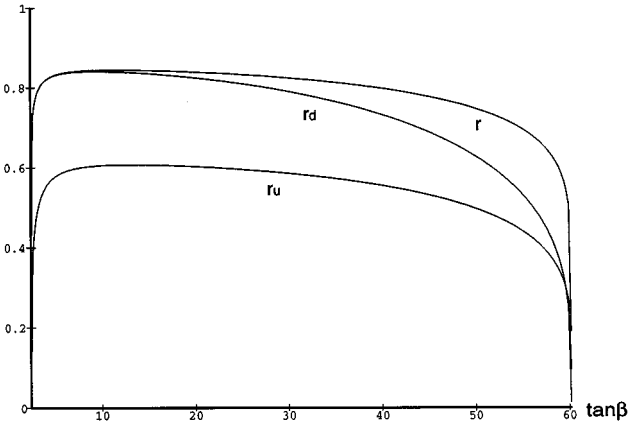
$$r = \exp\left(-\frac{1}{16\pi^2} \int_{\ln m_t}^{\ln m_G} \{\lambda_u^2(\mu) + \lambda_d^2(\mu)\} d \ln \mu\right). \quad (7)$$

The $\lambda(\mu)$'s in these expressions are furthermore determined from the RGE's

$$\begin{aligned} \frac{d\lambda_u}{d \ln \mu} &\simeq \frac{1}{(4\pi)^2} \{6\lambda_u^2 + \lambda_d^2 - c_i g_i^2\} \lambda_u, \\ \frac{d\lambda_d}{d \ln \mu} &\simeq \frac{1}{(4\pi)^2} \{6\lambda_d^2 + \lambda_u^2 + \lambda_e^2 - c'_i g_i^2\} \lambda_d, \\ \frac{d\lambda_e}{d \ln \mu} &\simeq \frac{1}{(4\pi)^2} \{4\lambda_e^2 + 3\lambda_d^2 - c''_i g_i^2\} \lambda_e, \\ \frac{dg_i}{d \ln \mu} &\simeq \frac{1}{(4\pi)^2} b_i g_i^3 \quad (i=1,2,3). \end{aligned} \quad (8)$$

Here, λ_e denotes the [3,3] matrix element of the lepton Yukawa matrix and $c_i = (13/15, 3, 16/3)$, $c'_i = (7/15, 3, 16/3)$, $c''_i = (9/5, 3, 0)$, $b_i = (33/5, 1, -3)$. The scale $m_G \simeq 10^{16}$ (GeV) is the unification point of the three-gauge couplings which we shall take to be $\alpha_i = (0.017, 0.033, 0.100)$ (with $\alpha_i \equiv g_i^2/4\pi$) following Ref. [5].

Further simplification is possible if one assumes that $\tan\beta \ll O(m_t/m_b)$, in which case the contributions of the λ_d and λ_e terms in Eq. (7) can be largely neglected and as a result, $r_d \simeq r$ and $r_u \simeq r^3$. In the same limit, the evolutions of λ_u and λ_d are given by

FIG. 1. Scaling parameters as functions of $\tan\beta$.

$$\begin{aligned} \lambda_u(\mu)/\lambda_u &\simeq \{\eta(\mu)\}^{1/2} \{1 - (3/4\pi^2)\lambda_u^2 I(\mu)\}^{-1/2}, \\ \lambda_d(\mu)/\lambda_d &\simeq \{\eta'(\mu)\}^{1/2} \{\lambda_u(\mu)/\lambda_u\}^{1/6} \{\eta(\mu)\}^{-1/12}, \end{aligned}$$

where

$$\eta(\mu) \equiv \prod_i \{\alpha_i/\alpha_i(\mu)\}^{c_i/b_i}, \quad \eta'(\mu) \equiv \prod_i \{\alpha_i/\alpha_i(\mu)\}^{c'_i/b_i},$$

and

$$I(\mu) \equiv \int_{\ln m_t}^{\ln \mu} \eta(\mu) d \ln \mu.$$

Expressed in terms of the above parameters and functions, one has

$$r \simeq \{\lambda_u(m_G)/\lambda_u\}^{-1/6} \{\eta(m_G)\}^{1/12}. \quad (9)$$

From these results one sees that $r \simeq 1$ except when λ_u approaches a small region defined by $\lambda_u \simeq 2\pi/\sqrt{3I(m_G)}$ where r rapidly drops to zero.

For large $\tan\beta$'s, the analysis becomes more involved and one has to rely upon numerical methods for solving Eq. (8) and evaluating the r 's in Eq. (7). Interestingly, the values of the r 's do not deviate much from being of order 1 unless $\tan\beta$ reaches near the value of m_t/m_b where they begin to drastically decrease again. For a qualitative understanding of this observation, we solve Eq. (8) with the assumption $\lambda_u = \lambda_d$ (corresponding to $\tan\beta = m_t/m_b$) while momentarily ignoring contributions from the leptonic sector. In this limit, we find

$$\lambda_u(\mu) \simeq \lambda_d(\mu) \propto \{1 - (3.5/4\pi^2)I(\mu)\}^{-1/2}$$

which yields approximately $\lambda_u(m_G), \lambda_d(m_G) \rightarrow \infty$. Referring moreover to the results in Eqs. (7) and (9), we have then $r_u \simeq r_d \simeq r^2$ with $r \rightarrow 0$.

For easy reference, we include in Fig. 1 a plot based on numerical solutions of Eqs. (7) and (8) subject to the boundary condition⁴ (at m_t)

$$m_t = \frac{v}{\sqrt{2}} \lambda_u \sin\beta, \quad m_b = \frac{v}{\sqrt{2}} \lambda_d \cos\beta, \quad m_\tau = \frac{v}{\sqrt{2}} \lambda_e \cos\beta,$$

⁴More detailed results of some related calculations based on two-loop RGE's can be found in Ref. [6].

TABLE II. Quark mass patterns with five texture zeros and their ‘‘predictions.’’ (The subleading terms Δ 's in the above expressions for $|V_{cs}|$ and $|V_{cb}|$ are relegated to Table III.)

	\tilde{M}_u	\tilde{M}_d	‘‘Prediction’’
1	$\begin{pmatrix} 0 & u_{12}\lambda^6 & 0 \\ u_{12}\lambda^6 & u_{22}\lambda^4 & 0 \\ 0 & 0 & u_{33} \end{pmatrix}$	$\begin{pmatrix} 0 & d_{12}\lambda^3 & 0 \\ d_{12}^*\lambda^3 & d_{22}\lambda^2 & d_{23}\lambda^2 \\ 0 & d_{23}\lambda^2 & d_{33} \end{pmatrix}$	$ V_{us} = \sqrt{m_d/m_s} \pm \Delta_{11} + O(\lambda^3)$ $ V_{ub} = V_{cb} \sqrt{m_u/m_c} \pm \Delta_{12} + O(\lambda^6)$
2	$\begin{pmatrix} 0 & u_{12}\lambda^6 & 0 \\ u_{12}\lambda^6 & 0 & u_{23}\lambda^2 \\ 0 & u_{23}\lambda^2 & u_{33} \end{pmatrix}$	$\begin{pmatrix} 0 & d_{12}\lambda^3 & 0 \\ d_{12}^*\lambda^3 & d_{22}\lambda^2 & d_{23}\lambda^2 \\ 0 & d_{23}^*\lambda^2 & d_{33} \end{pmatrix}$	$ V_{us} = \sqrt{m_d/m_s} \pm \Delta_{21} + O(\lambda^3)$ $ V_{ub} = V_{cb} \sqrt{m_u/m_c} \pm \Delta_{22} + O(\lambda^6)$
3	$\begin{pmatrix} 0 & 0 & u_{13}\lambda^4 \\ 0 & u_{22}\lambda^4 & 0 \\ u_{13}\lambda^4 & 0 & u_{33} \end{pmatrix}$	$\begin{pmatrix} 0 & d_{12}\lambda^3 & 0 \\ d_{12}^*\lambda^3 & d_{22}\lambda^2 & d_{23}\lambda^2 \\ 0 & d_{23}\lambda^2 & d_{33} \end{pmatrix}$	$ V_{us} = \sqrt{m_d/m_s} + \Delta_{31} + O(\lambda^3)$ $ V_{ub} = \sqrt{m_u/m_t} \pm \Delta_{32} + O(\lambda^6)$
4	$\begin{pmatrix} 0 & u_{12}\lambda^6 & 0 \\ u_{12}\lambda^6 & u_{22}\lambda^4 & u_{23}\lambda^2 \\ 0 & u_{23}\lambda^2 & u_{33} \end{pmatrix}$	$\begin{pmatrix} 0 & d_{12}\lambda^3 & 0 \\ d_{12}^*\lambda^3 & d_{22}\lambda^2 & 0 \\ 0 & 0 & d_{33} \end{pmatrix}$	$ V_{us} = \sqrt{m_d/m_s} \pm \Delta_{41} + O(\lambda^3)$ $ V_{ub} = V_{cb} \sqrt{m_u/m_c} + \Delta_{42} + O(\lambda^6)$
5	$\begin{pmatrix} 0 & 0 & u_{13}\lambda^4 \\ 0 & u_{22}\lambda^4 & u_{23}\lambda^2 \\ u_{13}\lambda^4 & u_{23}\lambda^2 & u_{33} \end{pmatrix}$	$\begin{pmatrix} 0 & d_{12}\lambda^3 & 0 \\ d_{12}^*\lambda^3 & d_{22}\lambda^2 & 0 \\ 0 & 0 & d_{33} \end{pmatrix}$	$ V_{us} = \sqrt{m_d/m_s} \pm \Delta_{51} + O(\lambda^3)$ $ V_{ub} = \sqrt{m_u/m_c} \{ - V_{cb} ^2 + m_c/m_t \}^{1/2} + \Delta_{52} + O(\lambda^6)$

with $v \approx 246.2$ (GeV), $m_t \approx 175$ (GeV), $m_b \approx 2.78$ (GeV), and⁵ $m_\tau \approx 1.76$ (GeV).

III. GENERAL TEXTURE PATTERN OF NATURAL HERMITIAN QUARK MASS MATRICES

A. Parametrization of Hermitian quark mass matrices

Given the (scaled) diagonal quark mass matrices [1]

$$\tilde{M}_u^{\text{diag}}(m_t) = \begin{pmatrix} \xi_{ut}\lambda^7 & 0 & 0 \\ 0 & \xi_{ct}\lambda^4 & 0 \\ 0 & 0 & 1 \end{pmatrix},$$

$$\tilde{M}_d^{\text{diag}}(m_t) = \begin{pmatrix} \xi_{db}\lambda^4 & 0 & 0 \\ 0 & \xi_{sb}\lambda^2 & 0 \\ 0 & 0 & 1 \end{pmatrix}, \tag{10}$$

and the CKM matrix (in the standard form) [7]

$$V = \begin{pmatrix} c_1c_3 & s_1c_3 & s_3e^{-i\delta} \\ -s_1c_2 - c_1s_2s_3e^{i\delta} & c_1c_2 - s_1s_2s_3e^{i\delta} & s_2c_3 \\ s_1s_2 - c_1c_2s_3e^{i\delta} & -c_1s_2 - s_1c_2s_3e^{i\delta} & c_2c_3 \end{pmatrix}, \tag{11}$$

the most general Hermitian mass matrices can be constructed from

$$\tilde{M}_u = U \tilde{M}_u^{\text{diag}} U^\dagger, \tag{12}$$

$$\tilde{M}_d = D \tilde{M}_d^{\text{diag}} D^\dagger, \tag{13}$$

in which the unitary matrices U, D are subject to the constraint

$$U^\dagger D = \Phi_u V \Phi_d, \tag{14}$$

⁵Notice the end regions of the plot in Fig. 1 depend rather sensitively on the exact values of the numbers taken.

where $\Phi_{u,d}$ are some diagonal phase matrices. Furthermore, aside from a trivial quark-phase redefinition (which amounts

TABLE III. Expressions for the subleading terms in the last column of Table II.

$\Delta_{11} = \cos\delta \sqrt{\frac{m_u}{m_c}}$	$\Delta_{12} = \cos\delta \frac{\sqrt{m_d m_s}}{m_b} V_{cb} $
$\Delta_{21} = \cos\delta \sqrt{\frac{m_u}{m_c}}$	$\Delta_{22} = \cos\delta \frac{\sqrt{m_d m_s}}{m_b} \left(V_{cb} + \sqrt{\frac{m_c}{m_t}} \right)^a$
$\Delta_{31} = 0$	$\Delta_{32} = \cos\delta \frac{\sqrt{m_d m_s}}{m_b} V_{cb} $
$\Delta_{41} = \cos\delta \sqrt{\frac{m_u}{m_c}}$	$\Delta_{42} = 0$
$\Delta_{51} = \cos\delta \sqrt{\frac{m_u}{m_c}} \left(1 + \frac{m_c}{m_t} V_{cb} ^{-2} \right)^{-1/2}$	$\Delta_{52} = 0$

^aFor definiteness, we assume for this number the special case $\arg\{d_{23}\}=0$ and also $d_{23}>0$.

to $U \leftrightarrow \Psi U$ and $D \leftrightarrow \Psi D$, Ψ being some common phase matrix), one can always, for example, choose to parametrize the unitary matrices U, D according to

$$(i) \quad D \rightarrow D_s \quad \text{and then} \quad U^\dagger \rightarrow V \Phi D_s \quad (15)$$

or, somewhat analogously,

$$(ii) \quad U^\dagger \rightarrow U_s^\dagger \quad \text{and then} \quad D \rightarrow U_s \Phi' V, \quad (16)$$

where D_s, U_s^\dagger are the matrices D, U^\dagger written in the standard form (of V) after necessary rephasing, and Φ, Φ' are some diagonal phase matrices which can be arranged to have only two phases in each.

In what follows, we shall adopt prescription (ii) since we have found it to be more convenient for constructing natural mass matrices.⁶ Specifically, we let

$$\Phi' \equiv \begin{pmatrix} e^{i\phi} & 0 & 0 \\ 0 & e^{i\psi} & 0 \\ 0 & 0 & 1 \end{pmatrix} \quad (17)$$

and write, in terms of some orthogonal rotation matrices (C 's) and some diagonal phase matrices⁷ (Δ 's)

$$V = C_2 \Delta C_3 \Delta^\dagger C_1$$

and, accordingly,

$$U = C_{1u} \Delta_u C_{3u} \Delta_u^\dagger C_{2u}.$$

Defining three more orthogonal matrices $C_{id} \equiv C_{iu} C_i$ ($i=1,2,3$) we have, by Eq. (16),

$$D = \{C_{1d}\} \{C_1^\dagger (\Delta_u C_{3d} \Delta_u^\dagger) C_1\} \\ \times \{C_1^\dagger (\Delta_u C_3^\dagger \Delta_u^\dagger) (C_{2d} C_2^\dagger \Phi' C_2) (\Delta C_3 \Delta^\dagger) C_{1d}\}.$$

⁶Previously, in Ref. [1], we followed (i) to construct several mass pattern examples.

⁷See Ref. [1] for the precise definitions of the matrices introduced below.

B. Texture pattern of natural mass matrices

Following the procedure described in Ref. [1], we proceed to express V in the Wolfenstein parametrization [8] and likewise the matrices C 's as perturbative expansions in terms of the small parameter λ (Table I). Subsequently, we apply our ‘‘naturalness’’ criterion [1] on the resulting quark mass matrices to arrange for natural mass patterns. Below, we summarize our main result.

In terms of the CKM matrix parameters ($\lambda, A, \Lambda \equiv \sigma A/\lambda, \delta$), the quark mass ratios (ξ 's) and the free phases (ϕ, ψ) introduced in Eq. (17), natural Hermitian quark mass matrices exhibit the following general texture pattern:

$$\tilde{M}_u = \begin{pmatrix} u_{11} \lambda^7 & u_{12} \lambda^6 & u_{13} \lambda^4 \\ u_{12}^* \lambda^6 & u_{22} \lambda^4 & u_{23} \lambda^2 \\ u_{13}^* \lambda^4 & u_{23}^* \lambda^2 & u_{33} \end{pmatrix}, \quad (18)$$

$$\tilde{M}_d = \begin{pmatrix} d_{11} \lambda^4 & d_{12} \lambda^3 & d_{13} \lambda^4 \\ d_{12}^* \lambda^3 & d_{22} \lambda^2 & d_{23} \lambda^2 \\ d_{13}^* \lambda^4 & d_{23}^* \lambda^2 & d_{33} \end{pmatrix}, \quad (18)$$

with⁸

$$u_{11} = \xi_{ut} + \{\alpha^2 \xi_{ct} + |u_{13}|^2\} \lambda + O(\lambda^2),$$

$$u_{12} = \alpha \xi_{ct} + u_{13} u_{23} + O(\lambda^2),$$

$$u_{22} = \xi_{ct} + |u_{23}|^2 + O(\lambda^2),$$

$$u_{33} = 1 + O(\lambda^4),$$

$$d_{11} = \xi_{db} + |d_{12}|^2 / \xi_{sb} + O(\lambda^2),$$

$$d_{12} = \xi_{sb} \{e^{i(\phi-\psi)} + \alpha \lambda\} + O(\lambda^2),$$

⁸In specifying the values of quark masses or mass ratios we conventionally quote these numbers as being positive. In the expressions below and throughout the presentation of our results, however, quark masses m_q 's (and, in general, quark mass ratios ξ 's as well) can be chosen to have either positive or negative sign, depending upon the context of expressions they are in.

TABLE IV. Numerical estimates for the CKM “predictions” of the five texture-zero patterns. [Numbers in the curly brackets are results incorporating the additional constraint of Eq. (2).]

	λ	σ
1	$(0.23 \pm 0.05) + (0.06 \pm 0.01)\cos\delta$ { $(0.23 \pm 0.01) + (0.06 \pm 0.01)\cos\delta$ }	$(0.27 \pm 0.05) + (0.03 \pm 0.01)\cos\delta$ { $(0.27 \pm 0.05) + (0.03 \pm 0.01)\cos\delta$ }
2	$(0.23 \pm 0.05) + (0.06 \pm 0.01)\cos\delta$ { $(0.23 \pm 0.01) + (0.06 \pm 0.01)\cos\delta$ }	$(0.27 \pm 0.05) + (0.08 \pm 0.03)\cos\delta$ { $(0.27 \pm 0.05) + (0.08 \pm 0.03)\cos\delta$ }
3	0.23 ± 0.05 { 0.23 ± 0.01 }	$(0.42 \pm 0.07) + (0.03 \pm 0.01)\cos\delta$ { $(0.42 \pm 0.07) + (0.03 \pm 0.01)\cos\delta$ }
4	$(0.23 \pm 0.05) + (0.06 \pm 0.01)\cos\delta$ { $(0.23 \pm 0.01) + (0.06 \pm 0.01)\cos\delta$ }	0.27 ± 0.05 { 0.27 ± 0.05 }
5	$(0.23 \pm 0.05) + (0.03 \pm 0.01)\cos\delta$ { $(0.23 \pm 0.01) + (0.03 \pm 0.01)\cos\delta$ }	0.32 ± 0.08 { 0.32 ± 0.08 }

$$\begin{aligned}
 d_{13} &= u_{13} + \alpha A e^{i\psi} + \Lambda e^{i(\phi-\delta)} - d_{12}d_{23}\lambda + O(\lambda^2), \\
 d_{22} &= \xi_{sb} + O(\lambda^2), \\
 d_{23} &= u_{23} + A e^{i\psi} + O(\lambda^2), \\
 d_{33} &= 1 + O(\lambda^4). \tag{19}
 \end{aligned}$$

The remaining matrix element parameters in Eq. (18) are not fixed, but are constrained by our requirement of “naturalness” to

$$|u_{13}|, |u_{23}|, \alpha \leq 1. \tag{20}$$

The quark mass matrices of Eq. (18), although defined apparently at the scale of m_t , can, nonetheless, be implemented at any energy scale so long as one properly takes into account the renormalization group (RG) evolution of the quark mass ratios and the CKM parameters in Eq. (19).

IV. APPLICATIONS

A. Mass pattern viability check

Given any natural mass pattern, once written in the form of Eq. (18), one can examine its viability using Eqs. (19) and (20). Specifically, the matrix elements of the pattern must, to a good approximation, obey the following constraints:

$$\begin{aligned}
 |u_{22} - |u_{23}|^2 &\simeq \xi_{ct}, \\
 d_{22} &\simeq \xi_{sb}, \\
 |d_{23} - u_{23}| &\simeq A, \\
 |d_{12}/\xi_{sb} - (u_{12} - u_{13}u_{23})\lambda/\xi_{ct}| &\simeq 1, \\
 |d_{13} - u_{13} - (d_{23} - u_{23})(u_{12} - u_{13}u_{23})/\xi_{ct} + d_{12}d_{23}\lambda| &\simeq \Lambda, \\
 u_{11} - |u_{13}|^2\lambda - (|u_{12} - u_{13}u_{23}|^2/\xi_{ct})\lambda - \xi_{ut} &\simeq 0, \\
 d_{11} - (\xi_{db} + |d_{12}|^2/\xi_{sb}) &\simeq 0,
 \end{aligned}$$

$$\begin{aligned}
 &\arg\{d_{13} - u_{13} - (d_{23} - u_{23})(u_{12} - u_{13}u_{23})/\xi_{ct} + d_{12}d_{23}\lambda\} \\
 &- \arg\{d_{12}/\xi_{sb} - (u_{12} - u_{13}u_{23})\lambda/\xi_{ct}\} - \arg\{d_{23} - u_{23}\} \simeq -\delta. \tag{21}
 \end{aligned}$$

As an illustrative example, we apply the results of Eq. (21) to the study of a mass pattern, recently proposed [9], based on the idea of a “democratic” symmetry. In this model, after some straightforward manipulations, the quark mass matrices take the form

$$\begin{aligned}
 M_u &\simeq m_t \begin{pmatrix} 0 & u & 0 \\ u & \frac{2}{9}\epsilon_u & -\frac{\sqrt{2}}{9}\epsilon_u \\ 0 & -\frac{\sqrt{2}}{9}\epsilon_u & 1 \end{pmatrix}, \\
 M_d &\simeq m_b \begin{pmatrix} 0 & d e^{i\omega} & 0 \\ d e^{-i\omega} & \frac{2}{9}\epsilon_d & -\frac{\sqrt{2}}{9}\epsilon_d \\ 0 & -\frac{\sqrt{2}}{9}\epsilon_d & 1 \end{pmatrix},
 \end{aligned}$$

where the symmetry-breaking parameters $u \ll \epsilon_u \ll 1$ and $d \ll \epsilon_d \ll 1$ are to be determined from the known values of quark masses. Using the expressions of Eq. (21), one finds $\epsilon_u \simeq (9/2)\xi_{ct}\lambda^4$, $\epsilon_d \simeq (9/2)\xi_{sb}\lambda^2$, $u \simeq \sqrt{\xi_{ut}\xi_{ct}}\lambda^{11/2}$, $d \simeq \sqrt{\xi_{db}\xi_{sb}}\lambda^3$, and, furthermore, the following relations which can be regarded as the CKM “predictions” of the pattern:

$$\begin{aligned}
 \lambda &\simeq \sqrt{m_d/m_s} \pm \cos\omega \sqrt{m_u/m_c}, \\
 A\lambda^2 &\simeq (m_s/m_b - m_c/m_t)/\sqrt{2}, \\
 \sigma A\lambda^3 &\simeq (m_s/m_b - m_c/m_t)\sqrt{m_u/2m_c},
 \end{aligned}$$

TABLE V. Quark mass patterns which may be useful as templates. $[(A, B, \dots, F)$ are fixed parameters of order 1 and (x, y, z) 's are adjustable parameters.]

	\tilde{M}_u	\tilde{M}_d
1	$\begin{pmatrix} \leq O(\lambda^9) & \leq O(\lambda^6) & y_u B e^{-i\phi_u} \lambda^4 \\ \leq O(\lambda^6) & B \lambda^4 & x_u B \lambda^4 \\ y_u B e^{i\phi_u} \lambda^4 & x_u B \lambda^4 & A \end{pmatrix}$	$\begin{pmatrix} \leq O(\lambda^6) & F e^{-i\psi_d} \lambda^3 & y_d F e^{-i\phi_d} \lambda^3 \\ F e^{i\psi_d} \lambda^3 & E \lambda^2 & x_d E \lambda^2 \\ y_d F e^{i\phi_d} \lambda^3 & x_d E \lambda^2 & D \end{pmatrix}$
2	$\begin{pmatrix} C \lambda^7 & z_u C \lambda^7 & y_u B e^{-i\phi_u} \lambda^4 \\ z_u C \lambda^7 & B \lambda^4 & x_u B \lambda^4 \\ y_u B e^{i\phi_u} \lambda^4 & x_u B \lambda^4 & A \end{pmatrix}$	$\begin{pmatrix} \leq O(\lambda^6) & F e^{-i\psi_d} \lambda^3 & y_d F e^{-i\phi_d} \lambda^3 \\ F e^{i\psi_d} \lambda^3 & E \lambda^2 & x_d E \lambda^2 \\ y_d F e^{i\phi_d} \lambda^3 & x_d E \lambda^2 & D \end{pmatrix}$
3	$\begin{pmatrix} \leq O(\lambda^9) & C \lambda^6 & \leq O(\lambda^6) \\ C \lambda^6 & \leq O(\lambda^6) & B \lambda^2 \\ \leq O(\lambda^6) & B \lambda^2 & A \end{pmatrix}$	$\begin{pmatrix} \leq O(\lambda^6) & F e^{-i\psi_d} \lambda^3 & y_d F e^{-i\phi_d} \lambda^3 \\ F e^{i\psi_d} \lambda^3 & E \lambda^2 & x_d E \lambda^2 \\ y_d F e^{i\phi_d} \lambda^3 & x_d E \lambda^2 & D \end{pmatrix}$
4	$\begin{pmatrix} C \lambda^7 & z_u C \lambda^7 & \leq O(\lambda^6) \\ z_u C \lambda^7 & \leq O(\lambda^6) & B \lambda^2 \\ \leq O(\lambda^6) & B \lambda^2 & A \end{pmatrix}$	$\begin{pmatrix} \leq O(\lambda^6) & F e^{-i\psi_d} \lambda^3 & y_d F e^{-i\phi_d} \lambda^3 \\ F e^{i\psi_d} \lambda^3 & E \lambda^2 & x_d E \lambda^2 \\ y_d F e^{i\phi_d} \lambda^3 & x_d E \lambda^2 & D \end{pmatrix}$
5	$\begin{pmatrix} \leq O(\lambda^9) & \leq O(\lambda^8) & C \lambda^4 \\ \leq O(\lambda^8) & x_u C \lambda^4 & B \lambda^2 \\ C \lambda^4 & B \lambda^2 & A \end{pmatrix}$	$\begin{pmatrix} \leq O(\lambda^6) & F e^{-i\psi_d} \lambda^3 & y_d F e^{-i\phi_d} \lambda^3 \\ F e^{i\psi_d} \lambda^3 & E \lambda^2 & x_d E \lambda^2 \\ y_d F e^{i\phi_d} \lambda^3 & x_d E \lambda^2 & D \end{pmatrix}$

and $\delta \approx \omega + O(\lambda)$. One sees, when referring to the data in Table I, that this pattern leads to extremely low values for $|V_{cb}|$ and $|V_{ub}|$, although it has an acceptable value for the quantity $|V_{ub}/V_{cb}|$.

B. Mass patterns with most texture zeros

Starting with Eqs. (18)–(20), arranging for patterns with multiple texture zeros can be particularly efficient. As an exercise, we insert zeros in all entries of the mass matrices of Eq. (18) where possible. We find, in this way, a total of five allowable five texture-zero, low energy (at the scale of m_t) patterns. To ensure consistence with the LED, the matrix elements of these five texture-zero patterns are specified in accordance with Eq. (19). In Table II we list these patterns and their CKM constraints or ‘‘predictions.’’⁹

Numerically, with the signs of the quark masses and those of the Δ terms in Table II judiciously chosen, the CKM predictions of these patterns can be estimated using the quark mass ratios and the value of $|V_{cb}|$ given in Table I. As an example, in Table IV we give some results, corresponding to a certain possible choice of the aforementioned signs. In ad-

dition, we have also included estimates with the much more stringent constraint of Eq. (2) taken into account.

To implement the above five texture-zero patterns at the GUT scale in the MSSM, the only necessary modification required of Tables II and III is the insertion of the RG scaling factors (r_u 's, r_d 's, and r 's) in front of the quark mass ratios and the parameters V_{cb} and V_{ub} , based on Eqs. (3)–(6). Having done so, one sees that the CKM predictions of patterns 1, 2, and 4 are unaltered to the leading order in λ and, therefore, these patterns are also viable as SUSY GUT patterns; the same is true for patterns 3 and 5 for most values¹⁰ of $\tan\beta$. However, near the end regions of the plot in Fig. 1 (where, for example, $\tan\beta$ is very small), the $|V_{ub}|$ predictions of these patterns can become unsound. Incidentally, as it was observed in Ref. [10], the nearest conceivable six texture-zero SUSY GUT pattern corresponds to pattern 2 in Table II with the parameter d_{23} of \tilde{M}_d set to zero. As a result, this pattern generates an extra, but unfortunately, generally unfavorable, CKM ‘‘prediction’’ $|V_{cb}| = \{\sqrt{r_u/r^2}\} \sqrt{m_c/m_t} + O(\lambda^4)$ (since the ratio r_u/r^2 is typically close to 1 according to Fig. 1). Nonetheless, in light of our discussion on the evolution of the LED parameters, this six texture-zero pattern could still be viable, should the scenario in which $\tan\beta \ll O(m_t/m_b)$ (consequently, $r_u/r^2 \approx r$) and, furthermore, $r \approx O(\lambda)$ prevails.

⁹‘‘Predictions’’ ensue whenever certain matrix elements or parameters are overspecified [1]. For each of the mass patterns in Table II, for example, Eq. (19) renders two of the LED parameters dependent (chosen here to be λ and Λ or, equivalently, $|V_{us}|$ and $|V_{ub}|$) while the remaining ones are not overspecified and as a result, their experimental values can always be accommodated.

¹⁰This is consistent with the findings of Ref. [10] where these five texture-zero patterns, obtained through a detailed numerical analysis, were first presented.

TABLE VI. CKM ‘‘Predictions’’ of the patterns in Table V.

	$ V_{us} $	$ V_{cb} $	V_{ub}
1	$\sqrt{\frac{m_d}{m_s}}$ $\pm \cos\psi_d \sqrt{\frac{m_u}{m_c} + y_u^2 \frac{m_c}{m_t}}$ $+ O(\lambda^3)$	$x_d \frac{m_s}{m_b}$ $+ x_u \frac{m_c}{m_t}$ $+ O(\lambda^4)$	$\left\{ y_d \frac{\sqrt{m_d m_s}}{m_b} e^{-i\phi_d} + y_u \frac{m_c}{m_t} e^{-i\phi_u} \right.$ $\left. \pm \sqrt{\frac{m_u}{m_c} + y_u^2 \frac{m_c}{m_t}} V_{cb} \right\} e^{i\psi_d}$ $+ x_d \left(\frac{m_s}{m_b} \right)^2 V_{us} + O(\lambda^6)$
2	$\sqrt{\frac{m_d}{m_s}}$ $+ z_u \left(\frac{m_u}{m_c} + y_u^2 \frac{m_c}{m_t} \right) \cos\psi_d$ $+ O(\lambda^4)$	$x_d \frac{m_s}{m_b}$ $+ x_u \frac{m_c}{m_t}$ $+ O(\lambda^4)$	$\left\{ y_d \frac{\sqrt{m_d m_s}}{m_b} e^{-i\phi_d} + y_u \frac{m_c}{m_t} e^{-i\phi_u} \right.$ $\left. + z_u \left(\frac{m_u}{m_c} + y_u^2 \frac{m_c}{m_t} \right) V_{cb} \right\} e^{i\psi_d}$ $+ x_d \left(\frac{m_s}{m_b} \right)^2 V_{us} + O(\lambda^6)$
3	$\sqrt{\frac{m_d}{m_s}}$ $\pm \cos\psi_d \sqrt{\frac{m_u}{m_c}}$ $+ O(\lambda^3)$	$\sqrt{\frac{m_c}{m_t}}$ $- x_d \frac{m_s}{m_b}$ $+ O(\lambda^4)$	$\left\{ -y_d \frac{\sqrt{m_d m_s}}{m_b} e^{-i\phi_d} \right.$ $\left. \pm \sqrt{\frac{m_u}{m_c}} V_{cb} \right\} e^{i\psi_d}$ $+ x_d \left(\frac{m_s}{m_b} \right)^2 V_{us} + O(\lambda^6)$
4	$\sqrt{\frac{m_d}{m_s}}$ $+ z_u \frac{m_u}{m_c} \cos\psi_d$ $+ O(\lambda^4)$	$\sqrt{\frac{m_c}{m_t}}$ $- x_d \frac{m_s}{m_b}$ $+ O(\lambda^4)$	$\left\{ -y_d \frac{\sqrt{m_d m_s}}{m_b} e^{-i\phi_d} \right.$ $\left. + z_u \frac{m_u}{m_c} V_{cb} \right\} e^{i\psi_d}$ $+ x_d \left(\frac{m_s}{m_b} \right)^2 V_{us} + O(\lambda^6)$
5	$\sqrt{\frac{m_d}{m_s}}$ $+ \cos\psi_d \sqrt{\frac{m_u}{m_c} (1+w)}$ $+ O(\lambda^4)^a$	$\sqrt{\frac{m_c}{m_t} (1+w^{-1})}$ $- x_d \frac{m_s}{m_b}$ $+ O(\lambda^4)^a$	$\left\{ -y_d \frac{\sqrt{m_d m_s}}{m_b} e^{-i\phi_d} - \sqrt{\frac{m_u}{m_t} w} \right.$ $\left. + \sqrt{\frac{m_u}{m_c} (1+w)} V_{cb} \right\} e^{i\psi_d}$ $+ x_d \left(\frac{m_s}{m_b} \right)^2 V_{us} + O(\lambda^6)^a$

^aIn these expressions, w is defined to be the quantity $\{m_c^2/x_u^2 m_u m_t\}^{1/3}$ for notational brevity.

The detailed CKM ‘‘predictions’’ of the five patterns given here can be used to further speculate in favor of (or against) them, especially if experimental data becomes more precise. For instance, taking into account Eq. (2), one sees from Tables III and IV that for patterns 1, 2, and 4 to be successful, the CP phase δ must be quite large. The same is true for pattern 5, although to a slightly lesser degree. On the

other hand, pattern 3 imposes no such restriction; instead, it favors a somewhat larger $|V_{ub}|$ when compared to the rest.

C. Mass patterns useful as templates

By relating the matrix elements in Eq. (18) which may have similar orders of magnitude, one can search or arrange

for patterns that have fewer independent parameters and thus having potentially greater predictive power. Below, we provide five such simple quark mass patterns in Table V (and the CKM ‘‘predictions’’ of these patterns in Table VI) with the hope that they may be useful as templates for contemplating quark mass *Ansätze*.¹¹

In deriving the results of Tables V and VI, the parameters (x, y, z) ’s are assumed to be of order 1 or less, but are otherwise unspecified. This allows for certain flexibility in pattern fitting. Evidently, not all values for the (x, y, z) ’s work equally well; using Table VI and the LED of Table I, however, one can readily determine the feasibility of a given set of values for these adjustable parameters.

Certainly, construction of more elaborate patterns is also possible. But already, a host of interesting patterns can be obtained from Table V. In particular, notice that texture zeros can easily be accommodated by inserting them where allowed or by selectively specifying some of the (x, y, z) ’s to be 0’s.¹² Similarly, equalities among matrix elements can be arranged by specifying some of the (x, y, z) ’s to be 1’s. As an illustrative example, let us choose in pattern 2, $y_d=0, x_u=y_u=z_u=x_d=1$, and $\psi_d=\pi$; the result is a rather simple-looking pattern in which

$$\tilde{M}_u = \begin{pmatrix} C\lambda^7 & C\lambda^7 & B\lambda^4 e^{-i\phi_u} \\ C\lambda^7 & B\lambda^4 & B\lambda^4 \\ B\lambda^4 e^{i\phi_u} & B\lambda^4 & A \end{pmatrix},$$

$$\tilde{M}_d = \begin{pmatrix} 0 & F\lambda^3 & 0 \\ F\lambda^3 & E\lambda^2 & E\lambda^2 \\ 0 & E\lambda^2 & D \end{pmatrix}.$$

As a low energy pattern, it gives, to a very good approximation, the CKM ‘‘predictions’’:

¹¹To implement these patterns at the GUT scale in the MSSM, one simply takes into account the RG scaling of the quark mass ratios and the CKM parameters in Table VI, in complete analogy to the previous case of five texture-zero patterns.

¹²In fact, the five texture-zero patterns of Table II can be gotten this way as well.

$$|V_{us}| \approx \sqrt{\frac{m_d}{m_s} - \frac{m_u}{m_c} - \frac{m_c}{m_t}}, \quad |V_{cb}| \approx \frac{m_s}{m_b} + \frac{m_c}{m_t}, \quad |V_{ub}| \approx \frac{m_c}{m_t},$$

and $\delta \approx \phi_u - \pi$ (which, of course, yields the correct value for δ automatically when ϕ_u is suitably chosen). To check the soundness of the above ‘‘predictions,’’ we input the quark mass ratios of Table I and find

$$|V_{us}| \approx 0.22 \pm 0.05,$$

$$|V_{cb}| \approx 0.030 \pm 0.009, \quad \text{and} \quad |V_{ub}| \approx 0.0034 \pm 0.0003$$

in reasonable agreement with the CKM data, also given in Table I. [If we incorporate Eq. (2) into the calculation of $|V_{us}|$ above, we have instead $|V_{us}| \approx 0.22 \pm 0.01$.] Correspondingly, as a SUSY GUT pattern, it predicts:

$$|V_{us}| \approx \sqrt{\frac{m_d}{m_s} - \frac{m_u}{m_c} - \{r_u\} \frac{m_c}{m_t}},$$

$$|V_{cb}| \approx \left\{ \frac{r_d}{r} \right\} \frac{m_s}{m_b} + \left\{ \frac{r_u}{r} \right\} \frac{m_c}{m_t}, \quad |V_{ub}| \approx \left\{ \frac{r_u}{r} \right\} \frac{m_c}{m_t},$$

and, again, $\delta \approx \phi_u - \pi$. Since for most values of $\tan\beta$, $r_d/r \approx 1$ and r_u/r is of order 1 (Fig. 1), one sees that these GUT pattern ‘‘predictions’’ are equally ‘‘sound,’’ with possible exceptions noted for extreme values of $\tan\beta$.

It is worth pointing out that using the results of Eqs. (18)–(20), the quark mass patterns of our examples are constructed in a completely systematic and often very efficient manner; moreover, ‘‘predictions’’ of these mass patterns are readily obtained in the form of explicit analytical expressions, making transparent the viability conditions of each pattern.

I would like to thank Professor Roberto Peccei for suggesting this project and for many valuable comments. This work was supported in part by the U.S. Department of Energy under Grant No. FG03-91ER40662.

[1] R. D. Peccei and K. Wang, Phys. Rev. D **53**, 2712 (1996).
 [2] D. Kaplan and A. Manohar, Phys. Rev. Lett. **56**, 2004 (1986); H. Leutwyler, Nucl. Phys. **B337**, 108 (1990).
 [3] H. Leutwyler, CERN Report No. CERN-TH/96-44 (unpublished).
 [4] K. Sasaki, Z. Phys. C **32**, 149 (1986); K. S. Babu, *ibid.* **35**, 69 (1987); M. Olechowski and S. Pokorski, Phys. Lett. B **257**, 388 (1991).
 [5] S. Dimopoulos, L. Hall, and S. Raby, Phys. Rev. D **45**, 4192 (1992); G. Anderson, S. Raby, S. Dimopoulos, and L. J. Hall, *ibid.* **47**, 3702 (1993).

[6] V. Barger, M. S. Berger, and P. Ohmann, Phys. Rev. D **47**, 1093 (1993).
 [7] Particle Data Group, L. Montanet *et al.*, Phys. Rev. D **50**, 1173 (1994).
 [8] L. Wolfenstein, Phys. Rev. Lett. **51**, 1945 (1983).
 [9] H. Fritzsch, in *B Physics Beyond the Standard Model at the B Factory*, Proceedings of the workshop, Nagoya, Japan, 1994, edited by A. I. Sanda and S. Suzuki (World Scientific, Singapore, 1995), p. 421; H. Fritzsch and Z. Xing, Phys. Lett. B **353**, 114 (1995).
 [10] P. Ramond, R. G. Roberts, and G. G. Ross, Nucl. Phys. **B406**, 19 (1993).